
SDG-TRACK: A HETEROGENEOUS OBSERVER–FOLLOWER FRAMEWORK FOR HIGH-RESOLUTION UAV TRACKING ON EMBEDDED PLATFORMS

A PREPRINT

Jiawen Wen
AI Thrust, HKUST(GZ)
jwen341@connect.hkust-gz.edu.cn

Yu Hu
School of Engineering, UBC
yuhu0424@gmail.com

Suixuan Qiu
Faculty of Geographical Science, BNU
qiusuixuan@mail.bnu.edu.cn

Jinshan Huang
FlyWin (Guangzhou) Technology Co., Ltd.
albert17official@gmail.com

Xiaowen Chu*
AI Thrust, HKUST(GZ)
xwchu@hkust-gz.edu.cn

December 5, 2025

ABSTRACT

Real-time tracking of small unmanned aerial vehicles (UAVs) on edge devices faces a fundamental resolution-speed conflict. Downsampling high-resolution imagery to standard detector input sizes causes small target features to collapse below detectable thresholds. Yet processing native 1080p frames on resource-constrained platforms yields insufficient throughput for smooth gimbal control. We propose SDG-Track, a Sparse Detection-Guided Tracker that adopts an Observer-Follower architecture to reconcile this conflict. The Observer stream runs a high-capacity detector at low frequency on the GPU to provide accurate position anchors from 1920x1080 frames. The Follower stream performs high-frequency trajectory interpolation via ROI-constrained sparse optical flow on the CPU. To handle tracking failures from occlusion or model drift caused by spectrally similar distractors, we introduce Dual-Space Recovery, a training-free re-acquisition mechanism combining color histogram matching with geometric consistency constraints. Experiments on a ground-to-air tracking station demonstrate that SDG-Track achieves 35.1 FPS system throughput while retaining 97.2% of the frame-by-frame detection precision. The system successfully tracks agile FPV drones under real-world operational conditions on an NVIDIA Jetson Orin Nano. Our paper code is publicly available at <https://github.com/Jeffry-wen/SDG-Track>

Keywords UAV tracking, edge computing, sparse detection, small object detection, embedded systems

1 Introduction

The growing use of unmanned aerial vehicles (UAVs) has increased the need for reliable systems that can detect and track them in real time. Unlike stationary radar installations, portable anti-UAV platforms face stringent Size, Weight, and Power (SWaP) constraints that mandate processing on embedded edge devices [1] such as the NVIDIA Jetson Orin Nano. Recent advances in edge computing have demonstrated promising results for UAV-based computer vision tasks [2]. However, deploying reliable tracking systems on these resource-constrained platforms remains a fundamental challenge.

*Corresponding author.

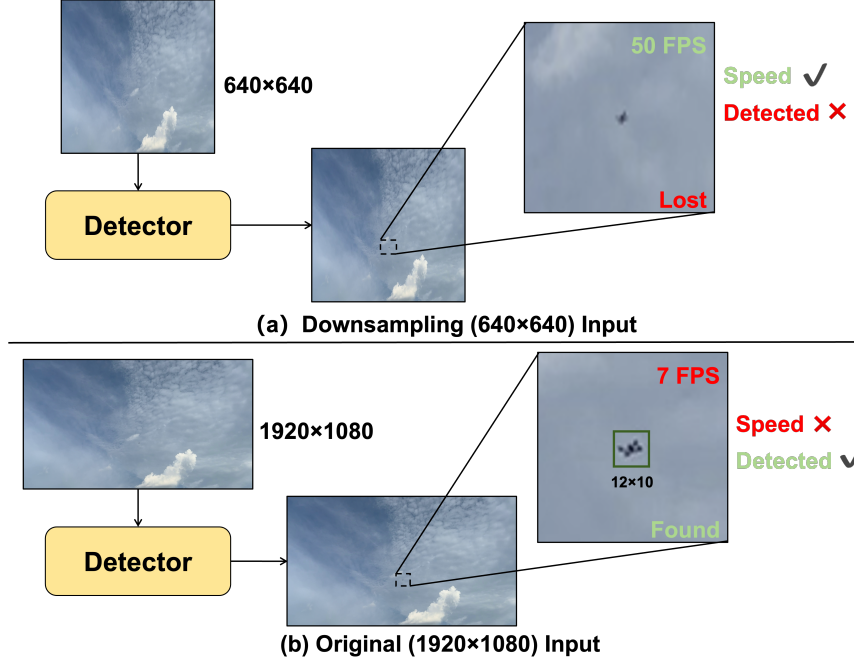


Figure 1: The inherent trade-off between detection resolution and inference speed on edge devices. (Top) Aggressive downsampling to 640×640 enables real-time performance (50 FPS) but results in the loss of critical spatial details, leading to detection failure. (Bottom) While maintaining the original 1920×1080 resolution allows the detector to resolve the small UAV target (12×10 pixels), the computational cost reduces the frame rate to ~ 7 FPS, failing to meet the requirements for smooth mechanical tracking.

The main difficulty arises from conflicting requirements for resolution and processing speed. Distant UAV targets often occupy fewer than 20×20 pixels in the image frame, with some objects as small as 4×4 pixels at extended ranges [3]. This creates what we term the vanishing pixel problem. When high-resolution imagery is downsampled to standard detection input sizes such as 640×640 , the spatial features of small distant objects collapse below recoverable thresholds (shown in Fig. 1). A target occupying 10×10 pixels in a 1080p frame shrinks to approximately 3×3 pixels after downsampling, it is too small to produce meaningful activations in early convolutional layers. The object’s signal effectively disappears from the feature maps, making detection impossible regardless of model architecture. This phenomenon necessitates high-resolution input, such as 1920×1080 , to preserve sufficient feature detail for small target detection. However, processing full HD imagery increases computational demands drastically. Our empirical profiling shows that even with TensorRT-FP16 optimization, state-of-the-art detectors like YOLOv11 [4] achieve less than 7 FPS on the Jetson Orin Nano when processing 1080p frames, which is far below the requirements for real-time tracking. Moreover, directly feeding such sparse, low-frequency detections to the gimbal controller induces mechanical oscillation and jitter, rendering smooth target pursuit impossible. Recent lightweight detection models have made progress on small object detection in aerial imagery. For instance, RemDet-Tiny achieves 37.6% mAP with only 3M parameters on the VisDrone2019 dataset [5], while SOD-YOLO improves detection speed through efficient backbone design [6]. Enhanced YOLOv11 variants have demonstrated 4.6% mAP improvement on VisDrone2019 by incorporating multi-scale context aggregation and scale-adaptive mechanisms [7]. However, these solutions optimize either for accuracy or speed. None achieve real-time performance on edge devices while processing the high-resolution imagery needed for small UAV detection.

The integration of optical flow for motion compensation has shown promise in various tracking contexts. The pyramidal Lucas-Kanade method provides efficient sparse optical flow computation [16]. Studies show that it has been successfully applied to vehicle tracking [17] and maritime object tracking [18]. Recent work demonstrates that sparse optical flow with moving window detection can maintain tracking with minimal computational overhead [19]. Hybrid approaches combining optical flow with detection have shown improvements in multi-object tracking scenarios [20] and autonomous vehicles [21]. However, existing flow-based approaches primarily focus on compensating for camera motion rather than exploiting flow as a primary mechanism for target state prediction during detector downtime. Additionally, ground-to-air (G2A) tracking presents drastic scale variations as FPV drones traverse the Z-axis toward or away from the camera, causing abrupt changes in target size that conventional trackers struggle to accommodate. Optical flow methods are also

susceptible to model drift when tracking against spectrally similar distractors such as drifting clouds, where purely visual features can mistake cloud edges for the aircraft, gradually pulling the tracker off-target. Furthermore, most methods apply flow densely across the entire frame, resulting in unnecessary computational overhead that undermines real-time performance on edge devices. To address these challenges, we propose Sparse Detection-Guided Tracker (SDG-Track), a heterogeneous tracking framework designed for edge deployment where high-resolution detection must operate at low frequency. Our approach adopts an Observer-Follower architecture that strategically partitions computation across available hardware resources. The Observer stream runs a lightweight YOLOv11 [4] detector at approximately 5 Hz on the GPU to provide periodic absolute position anchors and drift correction from high-resolution (1920×1080) frames. During inter-detection intervals, the Follower stream performs high-frequency trajectory interpolation via CPU-based sparse optical flow, operating strictly within a dynamically-sized Region of Interest (ROI) surrounding the last known target location. This ROI-constrained approach dramatically reduces the computational footprint to achieve real-time performance on limited CPU resources. To handle detection failures from occlusion or temporary target disappearance, we introduce Dual-Space Recovery, a training-free re-acquisition mechanism that fuses Lab and HSV color histograms with geometric consistency constraints, providing robust target recovery without the computational overhead of re-identification networks.

The contributions of this work are threefold. First, we present a sparse-detection TBD architecture that reconciles the resolution-speed conflict on resource-constrained edge platforms through strategic heterogeneous compute allocation. Second, we introduce an adaptive ROI-based motion compensation method that handles non-linear UAV trajectories with minimal CPU overhead by confining optical flow computation to task-relevant image regions. Third, we develop Dual-Space Recovery, a geometrically-constrained color matching approach for target re-acquisition that operates without learned embeddings. Experimental validation demonstrates that SDG-Track achieves 30+ FPS system throughput while maintaining state-of-the-art accuracy for small target tracking, deployed on a ground-to-air tracking station and tested against agile FPV drones under real-world operational conditions. This represents a significant advance in deployable edge-based UAV tracking systems.

Nam dui ligula, fringilla a, euismod sodales, sollicitudin vel, wisi. Morbi auctor lorem non justo. Nam lacus libero, pretium at, lobortis vitae, ultricies et, tellus. Donec aliquet, tortor sed accumsan bibendum, erat ligula aliquet magna, vitae ornare odio metus a mi. Morbi ac orci et nisl hendrerit mollis. Suspendisse ut massa. Cras nec ante. Pellentesque a nulla. Cum sociis natoque penatibus et magnis dis parturient montes, nascetur ridiculus mus. Aliquam tincidunt urna. Nulla ullamcorper vestibulum turpis. Pellentesque cursus luctus mauris. Nulla malesuada porttitor diam. Donec felis erat, congue non, volutpat at, tincidunt tristique, libero. Vivamus viverra fermentum felis. Donec nonummy pellentesque ante. Phasellus adipiscing semper elit. Proin fermentum massa ac quam. Sed diam turpis, molestie vitae, placerat a, molestie nec, leo. Maecenas lacinia. Nam ipsum ligula, eleifend at, accumsan nec, suscipit a, ipsum. Morbi blandit ligula feugiat magna. Nunc eleifend consequat lorem. Sed lacinia nulla vitae enim. Pellentesque tincidunt purus vel magna. Integer non enim. Praesent euismod nunc eu purus. Donec bibendum quam in tellus. Nullam cursus pulvinar lectus. Donec et mi. Nam vulputate metus eu enim. Vestibulum pellentesque felis eu massa.

2 Proposed Methodology

To achieve real-time tracking on limited edge hardware, we propose **SDG-Track**. This system uses an Observer-Follower design managed by a simple State Machine. As shown in Fig. 2, we split the workload to maximize efficiency: the GPU runs the *Observer Stream* at a low frame rate to correct tracking errors, while the CPU runs the *Follower Stream* at a high frame rate to track the target between detections. Additionally, if the target is lost, a *Recovery Module* combining Lab-HSV color models and geometric rules is automatically activated to find it again.

2.1 The Observer Stream

To prevent feature collapse, the *Observer Stream* processes native resolution (1920×1080) images rather than downsampling. While this increases computational load by $\sim 5\times$, it is essential for resolving small targets. Navigating the edge hardware trade-off between capacity and speed, we prioritize robustness by employing the heavy YOLO11-l over lightweight alternatives. Although this limits throughput to ~ 7 FPS on the Jetson Orin Nano, it ensures the detection precision required for distant targets.

To accommodate this latency, the detector operates asynchronously as shown in Fig. 2. These sparse outputs do not drive the control loop directly; instead, valid detections ($S_{det} > \tau_{det}$) serve as periodic anchors. They reset the tracker state B_{det} , effectively eliminating the drift accumulated by the high-frequency optical flow.

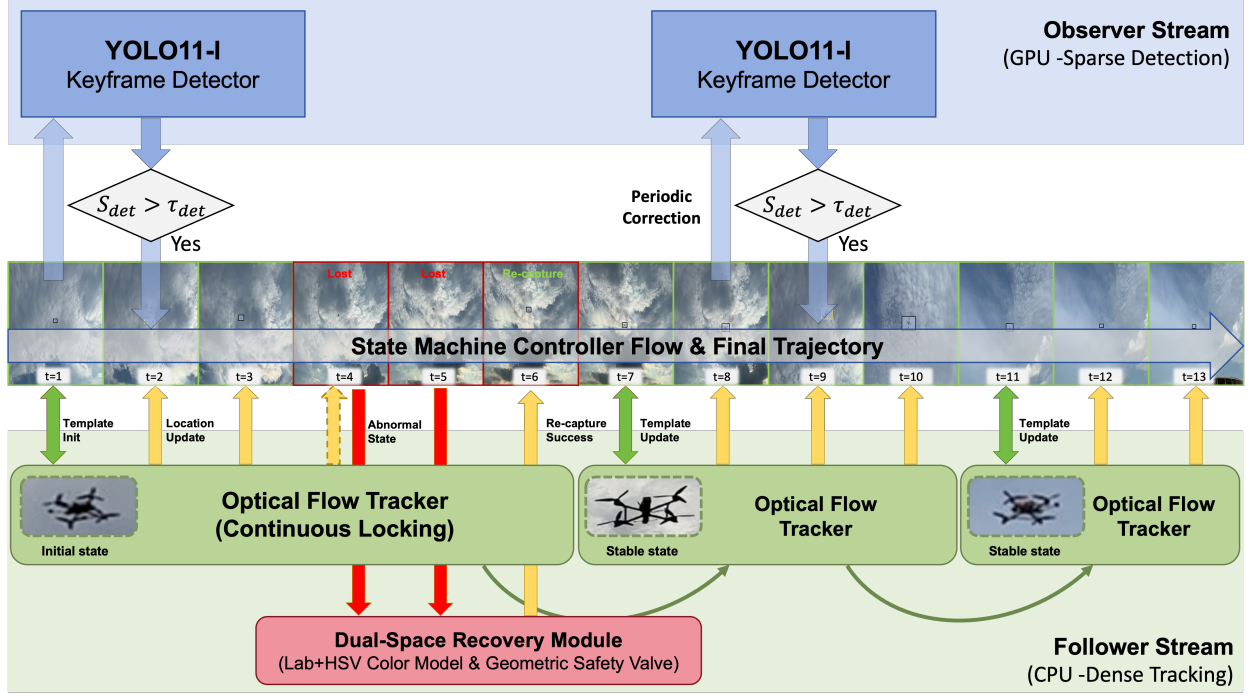


Figure 2: **Overview of the SDG-Track framework.** The architecture consists of three logical blocks: (1) An *Observer Stream* utilizing YOLO11-I (GPU) for periodic trajectory correction; (2) A **Follower Stream** using Optical Flow (CPU) for high-frequency tracking; and (3) A *Dual-Space Recovery Module* that leverages color and geometric constraints to handle target loss.

2.2 The Follower Stream

To bridge the frequency gap between the sparse detector and the high-speed PTZ control loop, the *Follower Stream* acts as a trajectory up-sampler. As shown in Fig. 3, this module is not merely a gap-filler but a robust tracker integrating adaptive ROI constraints, dynamic parameter tuning, and drift mitigation mechanisms to ensure smooth mechanical control.

2.2.1 Sparse ROI-based Optical Flow

To ensure real-time CPU performance, computation is confined to a dynamic Region of Interest (ROI) centered on the target’s predicted state. Within this ROI, we track *Shi-Tomasi* features using the *Pyramidal Lucas-Kanade* (LK) algorithm. Outliers (e.g., cloud edges) are rejected via median flow filtering, and the target bounding box is updated by re-fitting the remaining inliers, allowing the tracker to adaptively resize during fast motion.

2.2.2 Scale-Aware Parameter Tuning

Fixed tracking parameters fail against the drastic scale variations typical of G2A scenarios. We implement dynamic tuning for the search window \mathcal{W} and feature quality \mathcal{Q} based on target area A_{target} :

$$(\mathcal{W}, \mathcal{Q}) = \begin{cases} (\mathcal{W}_{small}, \mathcal{Q}_{low}), & \text{if } A_{target} < \tau_{area} \\ (\mathcal{W}_{large}, \mathcal{Q}_{high}), & \text{otherwise} \end{cases} \quad (1)$$

Empirically, $\mathcal{W}_{small} = 5 \times 5$ minimizes background noise for tiny targets, while $\mathcal{W}_{large} = 21 \times 21$ captures broader motion context.

2.2.3 Drift Correction and Template Maintenance

To mitigate the cumulative error inherent in optical flow, we employ a dual-strategy mechanism (Fig. 3, middle):

- **Drift Correction:** Performs periodic template matching every N frames to rectify local alignment errors.

- **Lazy Template Update:** Prevents template contamination (e.g., from occlusion) by refreshing visual features only when the target geometry remains stable (fluctuation $< \epsilon_{stable}$) for $K = 50$ consecutive frames.

2.2.4 Trajectory Smoothing

A linear *Kalman Filter* with state vector $\mathbf{x} = [u, v, \dot{u}, \dot{v}, w, h]^T$ eliminates high-frequency jitter. It fuses optical flow measurements with motion priors to generate smooth coordinate outputs for the PTZ controller, ensuring continuity even during brief feature loss.

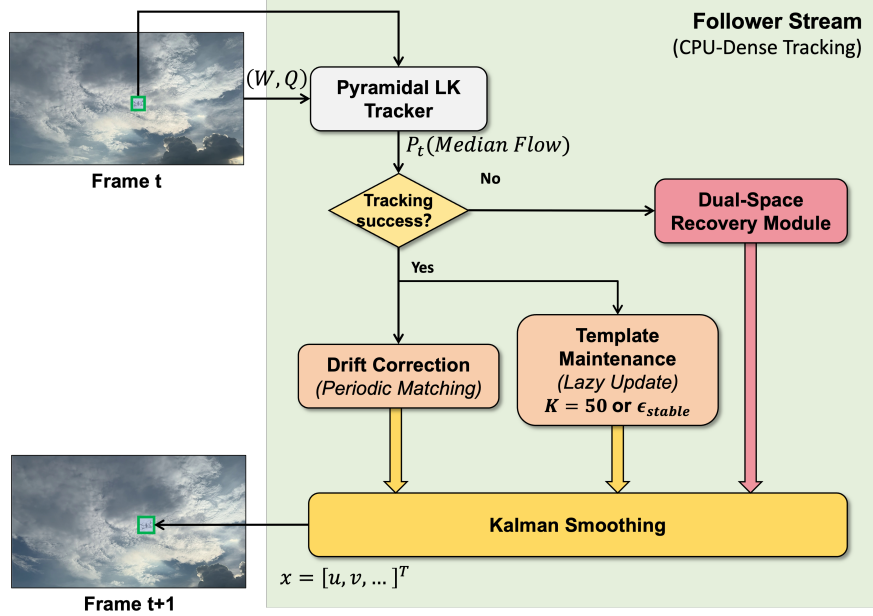


Figure 3: **Workflow of the Follower Stream.** The system enhances Pyramidal LK tracking with Median Flow filtering, *Drift Correction*, and *Lazy Template Update*. A Kalman Filter smooths the final trajectory for jitter-free control.

2.3 The Recovery Module: Constrained Dual-Space Re-localization

When both the detector and optical flow fail, the system enters the Recovery State. As illustrated in Fig. 4, we use a two-step process to re-capture the target without retraining: first, we generate a probability map using *Dual-Color Space Modeling*, and then we filter the results using a *Geometric Safety Valve*.

2.3.1 Dual-Color Space Modeling

Using a single color space is often unreliable due to lighting changes. To solve this, we first perform *Color Conversion* to map the input frame into two complementary spaces:

- **Lab Space (a/b Channels):** We calculate the Mahalanobis distance using only the a and b channels. By ignoring the L (Lightness) channel, the model remains stable even if the sky brightness changes. We denote this distance-based similarity map as M_{Lab} .
- **HSV Space (Back-Projection):** We use Histogram Back-Projection to check how well the pixels match the target’s hue distribution, generating a probability map denoted as M_{HSV} .

To fuse these maps, we employ an *Adaptive Weighting* strategy. The maps are combined via weighted summation: $M_{final} = \alpha M_{HSV} + \beta M_{Lab}$, where $\beta = 1 - \alpha$. The weight α is dynamically adjusted based on the target’s saturation: high saturation favors HSV, while low saturation relies more on Lab.

2.3.2 The Geometric Safety Valve

In G2A scenarios, pure color matching often yields false positives (e.g., clouds). To fix this, we apply the *Geometric Safety Valve*.

First, the fused probability map is processed by *OTSU Threshold Segmentation* to generate a discrete binary mask. This step automatically determines the optimal separation between target and background pixels without manual tuning.

Subsequently, the *Safety Valve* extracts contours from the binary mask and evaluates them against strict priors. Candidates are ranked by a composite score fusing the five constraints listed in the figure:

- **Color & HSV:** Verify spectral consistency with the target template.
- **Size:** Penalizes candidates with unrealistic scale changes compared to the previous frame.
- **Pre-Position:** Favors candidates spatially close to the last known location.
- **Shape:** Checks contour solidity to filter out irregular artifacts like wispy cloud edges.

Finally, the candidate with the highest score is accepted only if it exceeds a strict confidence threshold (set to 0.4), ensuring that weak matches are rejected.

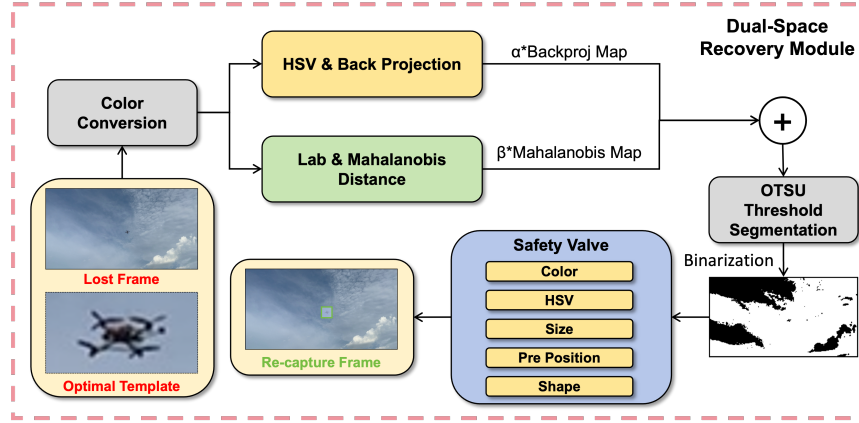


Figure 4: **Workflow of the Dual-Space Recovery Module.** The module fuses HSV and Lab probability maps using adaptive weights (α, β). A binary mask is generated via *OTSU segmentation*. Finally, the **Geometric Safety Valve** filters candidates based on a composite score of five constraints: *Color, HSV, Size, Previous Position, and Shape*, ensuring robust re-capture.

3 Experiments

We validate **SDG-Track** on edge platforms, beginning with the experimental setup and an analysis of accuracy-latency trade-offs to justify our backbone selection. We then present comparative results against state-of-the-art baselines and ablation studies to verify component contributions.

3.1 Experimental Setup

Implementation Details. We deploy the system on an **NVIDIA Jetson Orin Nano (8GB)**, optimizing all backbones via TensorRT (FP16). To ensure recall for small targets, we prioritize resolution over raw speed by processing inputs at their native 1920×1080 dimensions.

Data Collection Platform. We constructed a Ground-to-Air (G2A) tracking station (Fig. 5) comprising three core components:

- **Sensor:** Hikvision DS-2DE4A425IW-DE(S6), a Network PTZ camera streaming at 1080p.
- **Edge Node:** Jetson Orin Nano, executing the tracking algorithm and closing the PTZ control loop.
- **Target:** A custom FPV Drone simulating non-cooperative, high-dynamic aerial threats.

Datasets. We evaluate SDG-Track on two distinct datasets:

- **LRDD v2 [22]:** A public benchmark for long-range UAV tracking, serving as a standard testbed for tiny target detection.

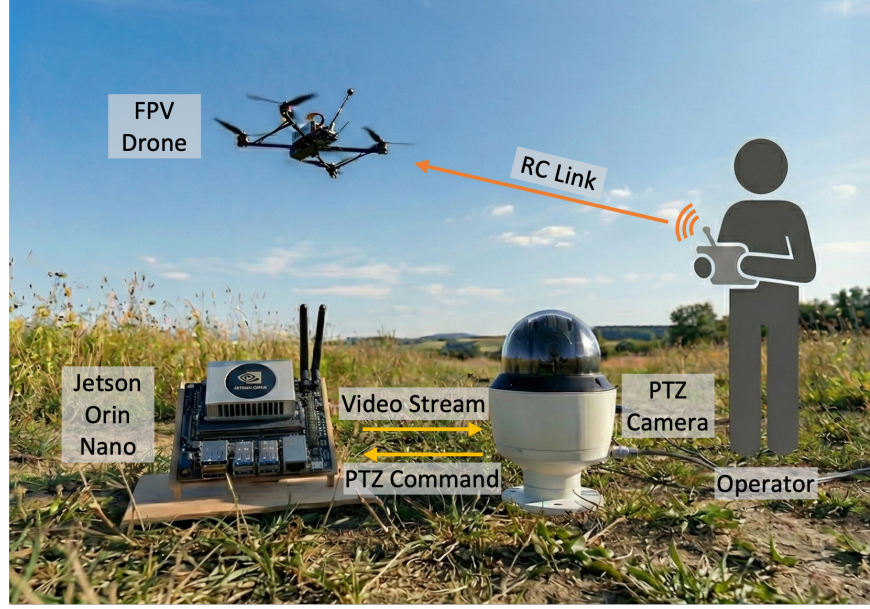


Figure 5: **Hardware setup of the G2A tracking station.** The Jetson Orin Nano processes 1080p streams from the PTZ camera and generates real-time control commands to track agile FPV drones.

- **Self-Collected Dataset:** Comprises 8 sequences (**11,327 frames**) captured at 1920×1080 using our platform, representing real-world deployment conditions.

Evaluation Metrics. Following standard protocols [22], we report:

- **Precision (Prec):** The percentage of frames with a Center Location Error (CLE) < 20 pixels.
- **Success (AUC):** The Area Under the Curve of the intersection-over-union (IoU) overlap plot.

3.2 Analysis of Inference Bottlenecks on Edge

Selecting the optimal detector backbone is a critical prerequisite for edge deployment. We benchmark the YOLO11 family (Nano to Extra-Large) on the Jetson Orin Nano to identify the upper bound of model capacity under real-time constraints.

Table 1: **Inference latency benchmark on Jetson Orin Nano.** The transition to 1920×1080 inputs causes a drastic FPS drop. **YOLO11l** is selected (*) as it represents the maximum model capacity feasible within the 8GB memory budget.

Model	Standard Input (640×640)	Native Input (1920×1080)
YOLO11n	120.6	23.8
YOLO11s	99.9	15.5
YOLO11m	61.4	8.6
YOLO11l	49.2	6.7*
YOLO11x	29.1	O.O.M.

As shown in Table 1, shifting from the standard input size (640×640) to the native sensor resolution (1920×1080) imposes a severe computational penalty. For instance, *YOLO11s* suffers an $\sim 84\%$ reduction in throughput. Crucially, at 1080p, the largest variant *YOLO11x* exceeds the 8GB memory limit (O.O.M.), establishing *YOLO11l* as the physical upper bound for model complexity on this platform.

Consequently, we select *YOLO11l* as the observer backbone. This decision represents a deliberate prioritization of semantic capacity over raw speed. Although lighter variants like *YOLO11n* achieve near real-time performance (23.8 FPS), they lack the parametric depth required to reliably distinguish tiny, distant drones from complex background

noise. By leveraging our dual-stream *Observer-Follower* architecture, we can effectively mitigate the low throughput of YOLO11l (6.7 FPS). The high-frequency Follower stream compensates for the temporal sparsity, allowing us to deploy the strongest feasible model to maximize detection recall without compromising the system’s overall control capability.

3.3 Comparative Analysis

We compare **SDG-Track** against standard tracking-by-detection (TbD) baselines (ByteTrack [23]) and alternative interpolation strategies. To ensure a fair comparison on the edge platform, we evaluate two distinct deployment strategies: (1) running the detector on every frame (Frame-by-Frame), and (2) using the sparse detection stream from YOLO11l (~ 150 ms intervals) and filling the gaps with lightweight trackers.

Table 2 summarizes the quantitative results on the Jetson Orin Nano. We compare our method against *ByteTrack* (using both Nano and Large backbones), a constant-velocity Kalman Filter predictor, and a *KCF* [24] tracker re-initialized at every detection.

Table 2: System-level quantitative comparison on Jetson Orin Nano.

Method	Backbone	Sys FPS	LRDD v2		Self-Collected	
			Prec	AUC	Prec	AUC
<i>Frame-by-Frame Tracking</i>						
ByteTrack	YOLO11n	22.6	0.412	0.285	0.453	0.310
ByteTrack	YOLO11l	6.1	0.915	0.682	0.897	0.665
<i>Sparse Detection + Interpolation</i>						
Kalman Predictor	YOLO11l	76.9	0.613	0.395	0.612	0.410
KCF	YOLO11l	56.7	0.594	0.418	0.745	0.532
SDG-Track (Ours)	YOLO11l	35.1	0.889	0.647	0.871	0.635

The results in Table 2 highlight the inherent conflict between recognition capability and inference speed on edge devices at 1920×1080 . Here, **Sys FPS** denotes the average offline *state-update/output rate* of the pipeline on recorded streams (including decoding and per-frame tracking). In the asynchronous setting, the detector runs *in parallel* and therefore does not throttle the per-frame update loop, enabling high-rate outputs.

Standard frame-by-frame tracking is fundamentally bounded by detector throughput. Even the fastest frame-by-frame configuration, *ByteTrack*+*YOLO11n*, only reaches 22.6 FPS and yields poor accuracy (Prec = 0.412), indicating that a lightweight detector is insufficient for tiny long-range drones. Conversely, *ByteTrack*+*YOLO11l* provides the strongest recognition (Prec = 0.915 / AUC = 0.682) but operates at a prohibitively slow 6.1 FPS, making it unsuitable for sustained 30 Hz PTZ control updates.

To utilize the high-precision *YOLO11l* backbone under real-time constraints, inter-frame interpolation becomes necessary. Given the ~ 150 ms blind interval between detections, naive interpolation strategies exhibit clear limitations. The *Kalman Predictor* achieves the highest output rate (76.9 FPS) due to its minimal per-frame cost, but its constant-velocity assumption breaks under drone maneuvering, resulting in limited accuracy (Prec = 0.613). The *KCF* re-initialization strategy is also computationally efficient (56.7 FPS), yet it is prone to drift under rapid appearance/scale changes and background clutter, leading to degraded robustness on the challenging LRDD v2 benchmark (Prec = 0.594).

In contrast, our proposed **SDG-Track** bridges this frequency gap with a more expressive motion model. Although it introduces additional per-frame computation (35.1 FPS) due to adaptive optical flow and robust rejection/recovery mechanisms, it achieves a substantially higher accuracy: **Prec = 0.889 / AUC = 0.647** on LRDD v2. Notably, SDG-Track retains **97.2%** of the heavy detector’s frame-by-frame precision upper bound (0.889 vs. 0.915, a drop of only 0.026) while still sustaining >30 FPS output, which is sufficient for robust 30 Hz PTZ servo control.

3.4 Ablation Study

To validate the contribution of individual components in SDG-Track, we evaluate three progressively enhanced variants on the LRDD v2 benchmark. All experiments use the same sparse detection backbone (*YOLO11l-1080p*):

1. **Baseline (No Interpolation):** The detector outputs sparse keyframes at ~ 6.7 Hz. Between detections, the system employs a *Zero-Order Hold (ZOH)* strategy, assuming the target position remains static until the next update.

2. **+ Follower Stream:** Activates the *Follower Stream*. Beyond basic optical flow, this integrates *scale-aware parameter tuning*, *Median Flow outlier rejection*, and *Kalman smoothing* to robustly bridge detection gaps.
3. **+ Recovery Module (Full SDG-Track):** Further enables the *Constrained Dual-Space Re-localization* mechanism to handle drift and re-capture targets after feature loss.

As shown in Table 3, all variants share the same sparse observer *YOLO11l-1080p* running at $\sim 6\text{--}7$ Hz (i.e., a $\sim 150\text{--}165$ ms blind interval). Note that **Sys FPS** reports the offline *per-frame state-update/output throughput*: even the ZOH baseline outputs a state every frame, but it only receives new detections at the observer rate.

On LRDD v2, the ZOH baseline often fails on fast targets: within a single blind interval, the drone can traverse a large image distance, so holding the last detection becomes unreliable. Enabling the Follower Stream closes this gap with high-frequency motion interpolation, together with scale-aware parameter tuning, MedianFlow outlier rejection, and Kalman smoothing. This improves Precision from 0.652 to 0.854 and AUC from 0.462 to 0.621, at the cost of reduced throughput (84.2 FPS to 44.8 FPS).

Although optical flow is effective under approximately continuous motion, it can drift in visually challenging cases such as low-texture clouds, abrupt turns, or background distractors. The Recovery Module further addresses these failures by re-verifying the target and re-capturing it after feature loss via constrained dual-space re-localization. With this additional verification, throughput decreases from 44.8 FPS to 35.1 FPS, while Precision increases to 0.889 and AUC to 0.647. The final system still sustains over 30 FPS throughput, which is sufficient for real-time control.

Table 3: **Ablation study on LRDD v2 under the same sparse observer (YOLO11l-1080p).** We report end-to-end system throughput (**Sys FPS**, offline processing) and tracking accuracy (Prec/AUC).

Variant	Sys FPS	Prec	AUC
Baseline (ZOH, no interpolation)	84.2	0.652	0.462
+ Follower Stream (Optical Flow + refinements)	44.8	0.854	0.621
+ Recovery Module (Full SDG-Track)	35.1	0.889	0.647

4 Conclusions

This paper presented SDG-Track, a heterogeneous tracking framework for edge-based UAV tracking under strict computational constraints. The proposed Observer-Follower architecture decouples high-resolution detection from high-frequency state estimation. This design enables deployment of a high-capacity detector (YOLO11l at 1080p) while maintaining sufficient output rate for real-time gimbal control. The Follower stream bridges detection gaps through adaptive ROI-constrained optical flow with scale-aware parameter tuning and robust outlier rejection. The dual-Space Recovery addresses model drift and target loss without requiring learned re-identification networks. The results from the experiment on both public benchmarks and a self-collected ground-to-air dataset shows the effectiveness of our approach. SDG-Track achieves 0.889 Precision and 0.647 AUC on LRDD v2 at 35.1 FPS. Ablation studies verify that each module contributes meaningfully to the final performance. Future work will explore learned motion prediction to handle more aggressive maneuvers. We also plan to investigate multi-target extensions and integration with threat classification modules for complete counter-UAV systems.

References

- [1] M. Fiorio, R. Galatolo, and G. Di Rito, “Development and experimental validation of a sense-and-avoid system for a mini-uav. Drones 2025, 9, 96,” 2025.
- [2] J. Suo, X. Zhang, W. Shi, and W. Zhou, “E 3-uav: An edge-based energy-efficient object detection system for unmanned aerial vehicles,” *IEEE Internet of Things Journal*, vol. 11, no. 3, pp. 4398–4413, 2023.
- [3] C. Wang, Y. Han, C. Yang, M. Wu, Z. Chen, L. Yun, and X. Jin, “Cf-yolo for small target detection in drone imagery based on yolov11 algorithm,” *Scientific Reports*, vol. 15, no. 1, p. 16741, 2025.
- [4] G. Jocher and J. Qiu. “Ultralytics Yolo11”, 2024
- [5] C. Li, R. Zhao, Z. Wang, H. Xu, and X. Zhu, “Remdet: Rethinking efficient model design for uav object detection,” in *Proceedings of the AAAI Conference on Artificial Intelligence*, vol. 39, no. 5, pp. 4643–4651, 2025.
- [6] Y. Xiao and N. Di, “Sod-yolo: A lightweight small object detection framework,” *Scientific Reports*, vol. 14, no. 1, p. 25624, 2024.

- [7] L. Lu, D. He, C. Liu, and Z. Deng, “Masf-yolo: An improved yolov11 network for small object detection on drone view,” arXiv preprint arXiv:2504.18136, 2025.
- [8] N. Wojke, A. Bewley, and D. Paulus, “Simple online and realtime tracking with a deep association metric,” in 2017 IEEE international conference on image processing (ICIP), pp. 3645–3649, IEEE, 2017.
- [9] Y. Zhang, P. Sun, Y. Jiang, D. Yu, F. Weng, Z. Yuan, P. Luo, W. Liu, and X. Wang, “Bytetrack: Multi-object tracking by associating every detection box,” in European conference on computer vision, pp. 1–21, Springer, 2022.
- [10] A. Bewley, Z. Ge, L. Ott, F. Ramos, and B. Upcroft, “Simple online and realtime tracking,” in 2016 IEEE international conference on image processing (ICIP) pp. 3464–3468, IEEE, 2016.
- [11] D. K. Nishad, S. Khalid, D. Prakash, V. K. Singh, and P. Sahani, “Advanced algorithms for uav tracking of targets exhibiting start-stop and irregular motion,” Scientific Reports, vol. 15, no. 1, p. 30507, 2025.
- [12] P.-S. Wang, C.-H. Lin, and C.-T. Chuang, “Real-time object localization using a fuzzy controller for a vision-based drone,” Inventions, vol. 9, no. 1, p. 14, 2024.
- [13] F. Han, S. Jiang, J. Wu, B. Xu, J. Zhao, and F. Shen, “Real-time object tracking in the wild with siamese network,” Multimedia Tools and Applications, vol. 82, no. 16, pp. 24 327–24 343, 2023.
- [14] S. Jiang, B. Xu, J. Zhao, and F. Shen, “Faster and simpler siamese network for single object tracking,” arXiv preprint arXiv:2105.03049, 2021.
- [15] A. A. Kareem, D. A. Hammood, A. A. Alchalaby, and R. A. Khamees, “A performance of low-cost nvidia jetson nano embedded system in the real-time siamese single object tracking: A comparison study,” in International Conference on Computing Science, Communication and Security , pp. 296–310 Springer, 2022.
- [16] S. Al-Qudah and M. Yang, “Large displacement detection using improved lucas–kanade optical flow,” Sensors, vol. 23, no. 6, p. 3152, 2023.
- [17] L. Gokul, P. Adarsh, G. Gokuldath, M. Ponmalar, S. Aswini et al., “Lucas kanade based optical flow for vehicle motion tracking and velocity estimation,” in 2023 International Conference on Control, Communication and Computing (ICCC). pp. 1–6, IEEE, 2023.
- [18] D. K. Prasad, D. Rajan, L. Rachmawati, E. Rajabally, and C. Quek, “Video processing from electro-optical sensors for object detection and tracking in a maritime environment: A survey,” IEEE Transactions on Intelligent Transportation Systems, vol. 18, no. 8, pp. 1993–2016, 2017.
- [19] H. Choi, B. Kang, and D. Kim, “Moving object tracking based on sparse optical flow with moving window and target estimator,” Sensors, vol. 22, no. 8, p. 2878, 2022.
- [20] H. Liu, T. Xu, and X. Wu, “Mmot: Motion-aware multi-object tracking with optical flow,” in Proceedings of the 2022 11th International Conference on Computing and Pattern Recognition, , pp. 115–120, 2022.
- [21] M. A. Sormoli, M. Dianati, S. Mozaffari, and R. Woodman, “Optical flow based detection and tracking of moving objects for autonomous vehicles,” IEEE Transactions on Intelligent Transportation Systems, vol. 25, no. 9, pp. 12 578–12 590, 2024.
- [22] A. Rouhi, S. Patel, N. McCarthy, S. Khan, H. Khorsand, K. Lefkowitz, and D. Han, “LRDDv2: Enhanced Long-Range Drone Detection Dataset with Range Information and Comprehensive Real-World Challenges,” in *Proc. 2024 International Symposium of Robotics Research (ISRR)*, 2024, pp. 1–6.
- [23] Y. Zhang, P. Sun, Y. Jiang, D. Yu, F. Weng, Z. Yuan, P. Luo, W. Liu, and X. Wang, “ByteTrack: Multi-Object Tracking by Associating Every Detection Box,” in *Proc. European Conference on Computer Vision (ECCV)*, 2022, pp. 1–21.
- [24] J. F. Henriques, R. Caseiro, P. Martins, and J. Batista, “High-Speed Tracking with Kernelized Correlation Filters,” *IEEE Transactions on Pattern Analysis and Machine Intelligence*, vol. 37, no. 3, pp. 583–596, 2014.